Measuring brain critical dynamics to inform Brain-Computer Interfaces

Marie-Constance Corsi [1,*], Pierpaolo Sorrentino [2,*], Denis Schwartz [1], Nathalie George [1], Laurent Hugueville [1], Ari E. Kahn [3], Sophie Dupont [1], Danielle S. Bassett [3], Viktor Jirsa [2,**], Fabrizio De Vico Fallani [1,**]

* These authors contributed equally and are listed alphabetically, ** these authors co-supervised equally

1 Sorbonne Université, Institut du cerveau - Paris Brain Institute - ICM, Inserm, CNRS, APHP, Hôpital de la Pitié Salpêtrière, Aramis team and CENIR MEG-EEG, Paris, France

2 Institut de Neuroscience des Systèmes, Aix-Marseille University, Inserm, Marseille, France

3 University of Pennsylvania, Philadelphia, USA

Abstract

Large-scale interactions among multiple brain regions manifest as bursts of activations, called neuronal avalanches, which reconfigure according to the task at hand and, hence, might constitute natural candidates to design brain-computer interfaces (BCI). To test this hypothesis, we compared source-reconstructed magneto/electroencephalography during resting-state and a motor imagery task performed within a BCI protocol. For each condition, we defined an individual avalanche transition matrix, tracking the probability that an avalanche would spread across any two regions. The edges whose transition probabilities significantly differed between conditions hinged selectively on premotor regions in all subjects, defining a topography related to the task. Furthermore, the individual differences in the transition probabilities for edges between pre/motor regions and parietal ones positively related to the individual task performance. Our results show that the patterns of propagation of large-scale perturbations are related to behavior and can be used to inform brain-computer interfaces.

Introduction

Brain-Computer Interfaces (BCIs) constitute a promising tool for establishing direct communication and control from the brain over external effectors. However, the ideal features to design a BCI are unknown, since the underlying microscopic brain processes, and their reflection on brain signals, are poorly-understood (1). As a result, mastering non-invasive BCI systems remains a learned skill that yields suboptimal performance in ~30% of users, referred to as the "BCI inefficiency" phenomenon (2). Measuring the dynamical features that are relevant to the execution of a task and, as a consequence, may

improve BCI performance, remains an open challenge (1). Electromagnetic imaging data is dominated by 'bursty' dynamics, with fast, fat-tailed distributed, aperiodic perturbations, called "neuronal avalanches", traveling across the whole brain (3). Neuronal avalanches spread preferentially across the white-matter bundles (4), they are modified by neurodegenerative diseases (5), and they evolve over a manifold during resting-state, generating rich functional connectivity dynamics (6). Such rich dynamics are a major contributor to time-averaged functional connectivity (3, 7). Hence, the spreading of neuronal avalanches might be a correlate of the functional interactions among brain areas and, as such, we hypothesize that they could spread differently according to the task at hand, thereby providing a powerful and original marker to differentiate between behaviors. To test our hypothesis, we compared source-reconstructed magnetoencephalography (MEG) signals in resting-state (RS) and while performing a motor imagery (MI) task in a BCI protocol, in order to track the dynamical features related to motor imagery as compared to rest. We obtained the probabilities of each pair of regions as being recruited sequentially in an avalanche (4), compared these probabilities across MI and RS conditions edge- and subject-wise, and related the differences between the two conditions to the performance in the BCI task, as measured using the BCI classification accuracy.

Results

We used the spatio-temporal spreading of large aperiodic bursts of activations as a proxy for communications between pairs of regions. Within this framework, large-scale, higher-order perturbations are considered to mediate the interactions between brain regions. We tested for differences between the two experimental conditions (i.e. resting-state, RS, and motor imagery, MI) in the probabilities of any such perturbation to propagate across two brain regions. To this end, we built an avalanche transition matrix (ATM) for each subject, containing regions in rows and columns, and the probability that region j would activate at time (t+1), given that region i was active at time t, as the ijth entry. The differences in the probability of being sequentially recruited by an avalanche was used to track (subject- and edge-wise) the spatial propagation of the perturbations across the two experimental conditions. To validate the observed differences, for each subject and each edge, we built a null-model (Figure 1A) randomizing the labels of each trial (i.e. RS or MI) 10000 times, so as to obtain a null distribution of the differences expected by chance. These distributions were used to spot, individually, the edges that differed between the two conditions above chance level. The significances were corrected for multiple comparisons across edges using the Benjamini Hochberg (BH) correction (8). Following this step, we focused on the edges that were consistently significant across subjects (defined here as "reliable" edges). To achieve this, we randomized 10000 times, in each subject, the statistically significant edges (Figure 1B). This way, we identified the edges which differed significantly between the experimental conditions in a higher number of subjects than

expected at chance level ($p<0.05$, BH corrected across edges). Our results show that there is a set of edges, consistent across most subjects, across which large-scale perturbations propagate differently according to the experimental condition (Figure 2A).

We then checked if the significantly different edges would cluster over specific brain regions. To this end, we computed the expected number of significant edges incident on any region, given a random distribution (with a comparable density), and selected those regions with an above-chance number of significant edges clustered upon them (Figure 1B). Statistics were again corrected using BH, this time across regions. These "reliably different" edges cluster on premotor regions bilaterally and, particularly, the caudal middle frontal gyri bilaterally ($p<0.0001$, BH corrected). We then hypothesize that the differences in the spreading of large-scale perturbations would carry information about the processes in place to execute the task. To test this hypothesis, we related the differences in the transition probabilities between the two experimental conditions (in each subject, for every edge) to the individual BCI performance (defined as the proportion of trials in which the subject controlled the BCI device) in the MI task, as measured using the BCI score. Figure 2B shows the edges whose differences between conditions correlate the most with the BCI scores (the color code shows the intensities of the correlations, for visualization purposes only edges with correlations with p-values < 0.05 are shown). Firstly, for nearly every edge we observed a positive correlation. To help interpretation, we clustered all the edges according to functional regions (i.e., executive regions, pre/motor areas, parietal areas, temporal areas, occipital areas, (Figure 1C). That is, we computed the average Spearman's correlation over all the edges connecting any two functional regions (also including self-connections, i.e. edges which are comprised within a functional region). To check if the differences in edges transition which correlated to task performance clustered over certain functional areas above chance-level, we again built a null-model. To this end, for 10000 times, we randomly allocated edges correlation coefficients to functional areas and, each time, we computed the average. We compared the observed average correlation coefficient to the null distribution to obtain a significance value per functional area. Significance values were then corrected for multiple comparisons across all their combinations (i.e., 5x5, 25 p-values). Our results suggest that edges that significantly relate to BCI task performance hinge pre/motor areas and parietal areas ($p<0.0001$, See Figure 2B, D). Since we retrieved nearly exclusively positive correlations, our results capture that perturbations - in the form of avalanches - spread more often between premotor/motor areas and parietal areas when the subject is engaged in the motor-imagery task, as compared to resting-state condition. We replicated the analysis demonstrating the robustness to the choice of arbitrary parameters (supplementary material 1), and to the methodology and parcellation used (supplementary materials 2, 3).

Finally, we have performed the same pipeline as described above, this time using the power spectra and the phase locking-value, both of them in the theta, alpha and beta bands, as features to distinguish the motor imagery from the resting-state (supplementary materials 4).

Discussion

In this work, we set out to test if neuronal avalanches can track subject-specific changes induced by the execution of a task (i.e., motor imagery) in the large-scale brain dynamics. The working hypothesis was that meaningful communication among regions on the large-scale is intermittent, and it is best understood and measured in terms of aperiodic perturbations. Neuronal avalanches are inherently aperiodic and scale-free perturbations whose statistical parameters meet theoretical predictions from mean-field theory (9–11). In our data, we confirmed that the measured branching ratio is compatible with that of a system operating at criticality or near-criticality. We went on from there to test the basic idea that brain regions interact differently while performing different tasks. We reasoned that, if avalanches convey interactions occurring between regions, then their spreading should also be modified according to the task at hand. Such modifications should then be tracked by avalanche transition matrices and, in turn, might be exploited to design better brain computer interfaces. More specifically, such information could be considered either as potential predictors of BCI performance, to conceive tailored training programs, or as alternative features, to improve the classification performance. Indeed, our results identify, in an unsupervised manner, a number of functional links (i.e. edges) that are reliably more likely to be dynamically recruited during a motor imagery task as compared to resting state. The edges cluster over regions typically involved in motor planning and attention as expected with a motor imagery task. In fact, premotor areas are involved in the planning of motor actions, imagining of actions, allocating executive attention (12), as well as in the selection between competing visual targets (13), while parietal areas are notably involved, among other things, with the processing of sensitive input. A premotor-parietal network has been found to be specifically implicated with spatial imagery tasks, which is in line with our finding (14).

Identifying neural markers associated with BCI performance is crucial to design optimized and tailored BCI systems (15). Neurophysiological predictors of BCI scores are most commonly associated with power spectra (16) or, more recently, with time-averaged brain interactions (17). Accordingly, in the latter case regional connectivity strength (18) and the M/EEG multiplex core-periphery (19) of specific associative and somatosensory areas held predictive power over BCI performance in the same session.

Here, we related the differences between MI and RS in the probability of an avalanche consecutively recruiting two regions to the magnitude of BCI performance. We find mostly positive correlations, indicating that the more avalanches spread between premotor/motor and parietal regions during the task, the better the control of the BCI. This might be interpreted as interactions between pre/motor regions and

parietal ones underpin the successful execution of the task. This finding also suggests that the patterns of spreading of neuronal avalanches are behaviourally meaningful (20).

All in all, we applied a newly described framework to BCI, in order to quantify large-scale interactions across brain regions by directly tracking the spreading of activations as they happen (as opposed to quantifying dependencies over time intervals). Using this straight-forward approach (4), we reliably retrieve functional information related to the execution of a task at the subject-level, which was not possible using classical functional metrics (18). This is based on theoretical underpinnings derived from statistical mechanics, which posits that higher-order, long-range correlations would appear in a near-critical dynamical regime (9). In fact, it is important to notice that, by z-scoring each region and using a high-threshold we selected only the activity which is unlikely to be generated by a linear process and that, instead, refers to a first-order phenomenon. In doing so, we discarded most of the available signals. In practice, we have discarded roughly 90% of the data, applying a "spatio-temporal" filter, and only selecting those points in time and space where large-scale aperiodic perturbations were found. To provide a comparison with more standards techniques, we have used the same pipeline based on techniques that assume stationarity (and take the whole data into account), namely the power-spectra (containing local information) and the phase-locking value (estimating bivariate synchronization between brain regions). Importantly, both these techniques failed to reproduce any pattern of differences between the two conditions that was replicable at the individual level (see supplementary materials Fig. S4). However, In the same dataset, a previous work showed that the power-spectra could show differences at the group-level (18). The fact that we could find robust individual differences while discarding most data and that we failed to do so when taking the whole data into account suggests that focusing on higher-order perturbations might be useful to capture functionally-relevant processes and, in turn, to apply them to the design of BCI.

We replicated our results using different thresholds and binnings showing that they are resilient to these choices. Also, they can be replicated using different parcellation schemes, and using EEG signals, which is more widely available than MEG for BCI applications, thereby making our methodology to be applied in a wide variety of settings. All in all, extensive replications make it unlikely that our results could be due to arbitrary choices or limited to a specific methodology. Taken together, our findings could pave the way to innovative BCI protocols notably relying on the use of alternative features based on the ATMs. Our results revealed the crucial role of brain dynamics to identify potential predictors of the BCI performance. Such information should be considered in the future to predict the BCI training outcome.

Methods

Cohort & experiment description & data preprocessing

MEG data were recorded during a BCI training session performed by a group of 20 healthy subjects (27.5 ± 4.0 years old, 12 men) (*18*). The participants were instructed to control the vertical position of a moving cursor by modulating their neural activity via a motor imagery task. Anatomical information was obtained from Magnetic Resonance Imaging (MRI) imaging afterwards, whereby individual T1 were obtained and preprocessed for all participants (*21*). M/EEG data were processed using the Independent Component Analysis method (*22*), followed by the source reconstruction on the epoched data via the Boundary Element Method associated with the weighted Minimum Norm Estimate (*23*). For a complete description of the preprocessing steps, please refer to Ref. (*18*).

Data pipeline

Each source-reconstructed signal was z-scored (over time), thresholded, and set to 1 when above threshold, and to zero otherwise (threshold: z = |3|). Then, an avalanche was defined as starting when at least one region is above threshold, and as finishing when no region is active. For each avalanche, we estimated a transition matrix, structured with regions in rows and columns, and the ij-th edge is defined as the probability that regions j would be active at time t+1, given region i was active at time t. Then, for each subject, we obtained an average transition matrix (i.e. averaging edge-wise over all avalanches) for the baseline condition, and an average transition matrix for the motor imagery task. To ensure appropriate sampling (24), we have binned the data with bins ranging from 1 to 3 (stopping at three to avoid aliasing). To select the optimal binning, we looked at the branching ratio, since a branching ratio ∼ 1 typically indicates a process operating near a critical regime. The branching ratio is calculated as the geometrically averaged (over all the time bins) ratio of the number of events (activations) between the subsequent time bin (descendants) and that in the current time bin (ancestors) - eq.1, as:

$$\sigma_i = \prod_{j=1}^{N_{bin}-1} \left(\frac{n_{events}\,(j+1)}{n_{events}\,(j)}\right)^{\frac{1}{N_{bin}-1}} \qquad (1)$$

and then geometrically averaging it over all the avalanches - eq.2 (9).

$$\sigma = \prod_{i=1}^{N_{aval}} (\sigma_i)^{\frac{1}{N_{aval}}} \qquad (2)$$

where σi is the branching parameter of the i-th avalanche in the dataset, Nbin is the total amount of bins in the i-th avalanche, nevents (j) is the total number of events active in the j-th bin, and Naval is the total number of avalanches in each participant's recording.

In branching processes, a branching ratio of σ = 1 indicates critical processes with activity that is highly variable and nearly sustained, σ < 1 indicates subcritical processes in which the activity quickly dies out,

and $\sigma > 1$ indicates supercritical processes in which the activity increases as runaway excitation. The bin length equal to one sample yielded a $\sigma = 1$, hinting at the avalanches as occurring in the context of a dynamical regime near operating near criticality, was chosen for subsequent analyses.

To provide a comparison with standard feature extraction techniques, we computed the power spectra, via the Welch method with a window length of 1 s and a window overlap ratio of 50%, and the phase-locking value, as in (25).

Statistical analysis

For each subject, we computed the difference in the probability of a perturbation running across a given edge during resting-state and during the MI task. To statistically validate this, for each individual, we randomly shuffled the labels of the individual avalanches (i.e. each trial-specific transition matrix was randomly allocated to either resting-state and motor imagery). We performed this procedure 10000 times, obtaining, for each edge, the distribution of the differences given the null-hypothesis that the transition matrices would not capture any difference between the two conditions. We used the null distribution to obtain a statistical significance for each edge. The retrieved significances were Benjamini-Hochberg-corrected for multiple comparisons across edges (8). Following this procedure, we obtained for each patient, a matrix with the edges that significantly differed from the two conditions. We then looked at the concordance of such matrices across subjects, as to only focus on the edges that are reliably related to the task at hand. We have only selected those edges that were significant in a higher-than-chance number of subjects. Finally, we selected only those nodes that had more significantly different edges incident upon them, as compared to chance level. This way, we selected the areas whose involvement in large-scale dynamics is qualitatively different, in multiple subjects, between the two conditions (i.e. RS vs. MI task), and refer to these as the "task-specific" areas.

Then, we moved on to check what edges differed related to the BCI performance. To this end, we related, for each edge, the individual differences in the transition probabilities in the two experimental conditions to the individual BCI performances. We then grouped the edges according to functional areas, namely: executive areas, pre/motor areas, parietal areas, temporal areas, and occipital areas. To statistically validate this approach, for 10000 we have randomly allocated the edges to these groups and computed the average correlation coefficient at each iteration for each group of edges. We used these averages to build a null-distribution for each functional area, and used to have a statistical significance. Finally, these significances were corrected across functional regions using the BH correction for multiple comparison. We have repeated the correlation analysis without grouping the regions into functional areas but carrying out the correlation analysis for each region separately. In this case, no single region survived the BH correction (not shown).

Finally, we replicated our results using the Destrieux parcellation scheme (26) and using the electroencephalogram. Furthermore, we repeated the analysis changing the threshold to define active regions. Finally, while our results can be placed within the framework of critical dynamics, they hold regardless of the kind of dynamical regime in which the system had been operating. Hence, we tested the solidity of our approach changing the binning from 1 (i.e., no binning) to three. The code used to perform the analysis is publicly available at https://github.com/mccorsi/NeuronalAvalanches4BCI.git.

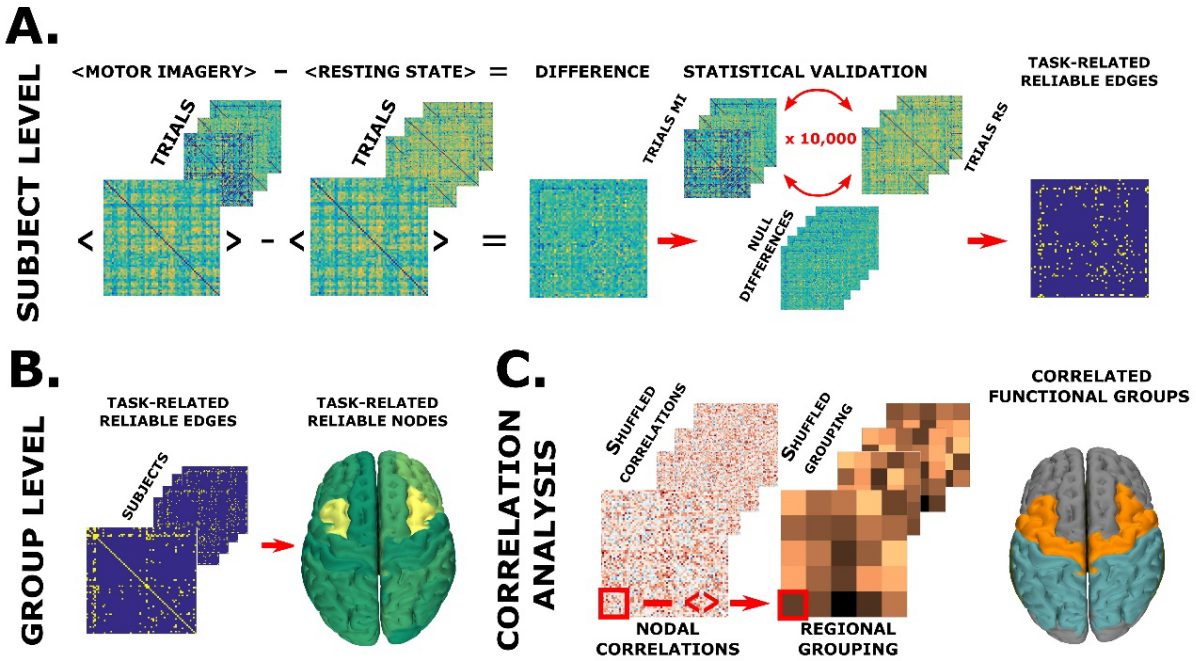

Figure 1 Overview of the analysis. A. Subject-level analysis: to identify, for each subject, the edges that show a significant condition effect. The average of all RS trials was subtracted, edge-wise, from the average of the MI trials. The differences were validated by shuffling the labels (i.e. MI and RS) 10000 times. This way, significantly different edges were identified for each patient. **B. Group level analysis:** we identified the edges that were significantly different in a large number of subjects (as compared to what would be expected by chance) and then performed nodal analysis to identify the regions over which significant differences were clustered. **C. Correlation analysis:** correlation coefficients between individual differences (for each edge) and individual BCI scores were averaged over 5 regions, namely, executive, pre/motor, parietal, temporal and occipital, obtaining one mean correlation between functional areas (i.e. 5 x 5 = 25 values). Then, the correlation coefficients were shuffled 10000 times, and each time surrogate average coefficients were obtained for each group of edges. These nulls were used to check if the edges with differences in transition probabilities that related to task performance clustered in any specific area. All statistical analyses were BH corrected for multiple comparisons, as appropriate.

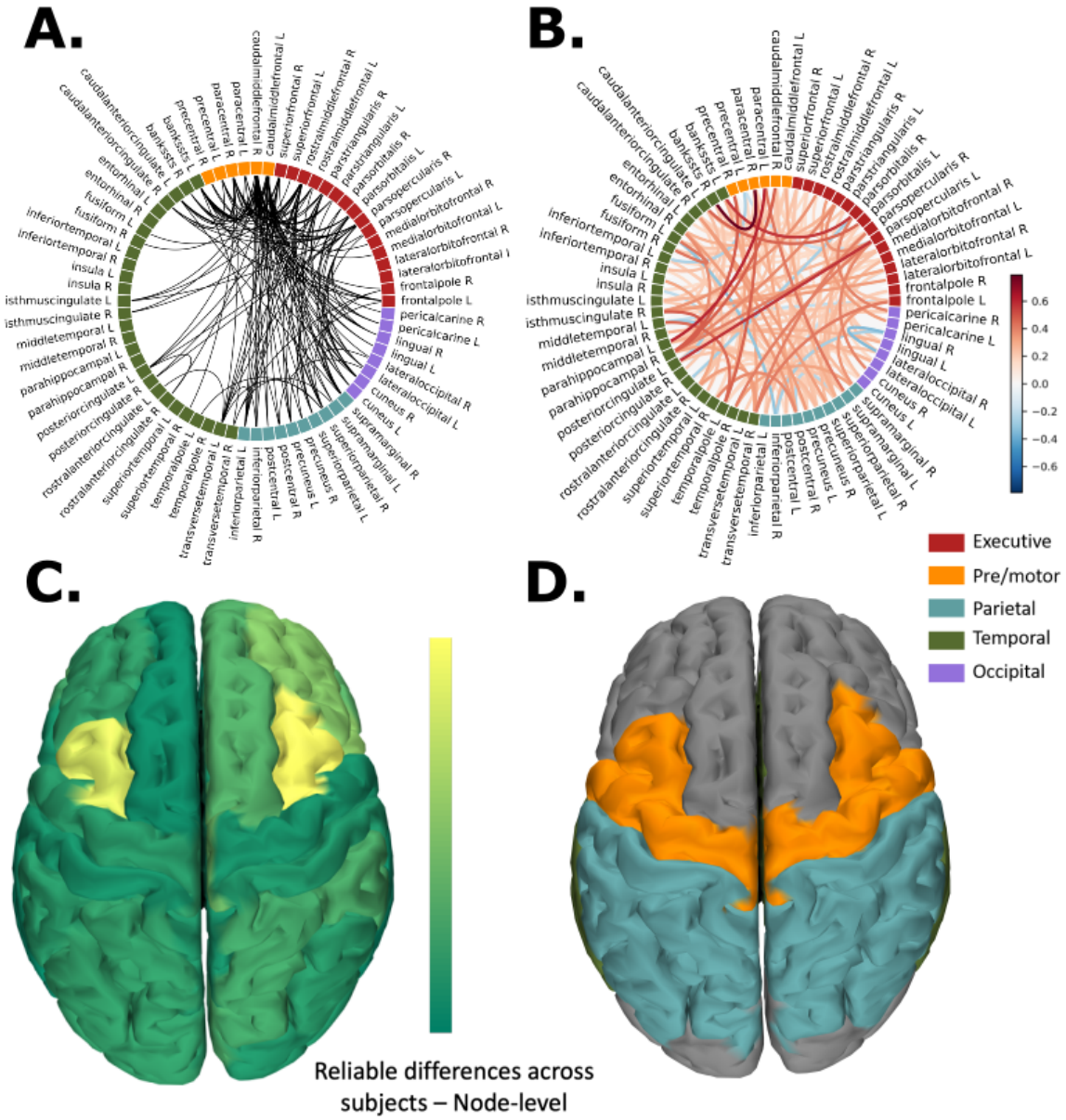

Figure 2 Main results. A. Edge-wise differences in transition probability: Reliably different task-based interactions over the subjects ($p<0.05$, after correction for multiple comparison). **B. Edge-wise correlations:** edge-wise correlation with BCI scores. For visualization purposes, only the edges with p-values<0.05 are visualized. The color of the edges is proportional to the correlation coefficient. **C. Node-wise differences in transition probabilities:** the colorscale is proportional to the nodal degree derived from the matrix with the group-significant differences (the brighter the color, the more edges that differ between tasks are clustered upon that node). **D. Node-wise differences in transition probabilities:** the picture shows the functional-areas averaged correlation coefficients. In orange the pre/motor areas, in turquoise the parietal lobe.

References

1. M. C. Thompson, Critiquing the Concept of BCI Illiteracy. *Sci Eng Ethics* (2018), doi:10.1007/s11948-018-0061-1.
2. B. Z. Allison, C. Neuper, in *Brain-Computer Interfaces*, D. S. Tan, A. Nijholt, Eds. (Springer London, 2010; http://link.springer.com/chapter/10.1007/978-1-84996-272-8_3), *Human-Computer Interaction Series*, pp. 35–54.
3. E. Tagliazucchi, F. Von Wegner, A. Morzelewski, V. Brodbeck, H. Laufs, Dynamic BOLD functional connectivity in humans and its electrophysiological correlates. *Frontiers in Human Neuroscience*. **6**, 339 (2012).
4. P. Sorrentino, C. Seguin, R. Rucco, M. Liparoti, E. Troisi Lopez, S. Bonavita, M. Quarantelli, G. Sorrentino, V. Jirsa, A. Zalesky, The structural connectome constrains fast brain dynamics. *eLife*. **10**, e67400 (2021).
5. P. Sorrentino, R. Rucco, F. Baselice, R. De Micco, A. Tessitore, A. Hillebrand, L. Mandolesi, M. Breakspear, L. L. Gollo, G. Sorrentino, Flexible brain dynamics underpins complex behaviours as observed in Parkinson's disease. *Sci Rep*. **11**, 4051 (2021).
6. G. Rabuffo, J. Fousek, C. Bernard, V. Jirsa, Neuronal Cascades Shape Whole-Brain Functional Dynamics at Rest. *eNeuro*. **8** (2021), doi:10.1523/ENEURO.0283-21.2021.
7. F. Z. Esfahlani, Y. Jo, J. Faskowitz, L. Byrge, D. P. Kennedy, O. Sporns, R. F. Betzel, High-amplitude cofluctuations in cortical activity drive functional connectivity. *PNAS*. **117**, 28393–28401 (2020).
8. Y. Benjamini, Y. Hochberg, Controlling the False Discovery Rate: A Practical and Powerful Approach to Multiple Testing. *Journal of the Royal Statistical Society. Series B (Methodological)*. **57**, 289–300 (1995).
9. P. Bak, C. Tang, K. Wiesenfeld, Self-organized criticality: An explanation of the 1/f noise. *Physical review letters*. **59**, 381 (1987).
10. L. Cocchi, L. L. Gollo, A. Zalesky, M. Breakspear, Criticality in the brain: A synthesis of neurobiology, models and cognition. *Progress in Neurobiology*. **158**, 132–152 (2017).
11. J. P. Sethna, K. A. Dahmen, C. R. Myers, Crackling noise. *Nature*. **410**, 242–250 (2001).
12. M. Andersson, M. Ystad, A. Lundervold, A. J. Lundervold, Correlations between measures of executive attention and cortical thickness of left posterior middle frontal gyrus - a dichotic listening study. *Behavioral and Brain Functions*. **5**, 41 (2009).
13. J. Germann, M. Petrides, Area 8A within the Posterior Middle Frontal Gyrus Underlies Cognitive Selection between Competing Visual Targets. *eNeuro*. **7** (2020), doi:10.1523/ENEURO.0102-20.2020.
14. A. T. Sack, C. Jacobs, F. D. Martino, N. Staeren, R. Goebel, E. Formisano, Dynamic Premotor-to-Parietal Interactions during Spatial Imagery. *J. Neurosci.* **28**, 8417–8429 (2008).
15. S. Perdikis, R. Leeb, J. del R. Millán, in *2014 36th Annual International Conference of the IEEE Engineering in Medicine and Biology Society* (2014), pp. 1259–1262.
16. M. Ahn, S. C. Jun, Performance variation in motor imagery brain–computer interface: A brief review. *Journal of Neuroscience Methods*. **243**, 103–110 (2015).
17. H. Sugata, M. Hirata, T. Yanagisawa, M. Shayne, K. Matsushita, T. Goto, S. Yorifuji, T. Yoshimine, Alpha band functional connectivity correlates with the performance of brain–machine interfaces to decode real and imagined movements. *Frontiers in Human Neuroscience*. **8** (2014) (available at https://www.frontiersin.org/article/10.3389/fnhum.2014.00620).
18. M.-C. Corsi, M. Chavez, D. Schwartz, N. George, L. Hugueville, A. E. Kahn, S. Dupont, D. S. Bassett, F. De Vico Fallani, Functional disconnection of associative cortical areas predicts performance during BCI training. *NeuroImage*. **209**, 116500 (2020).
19. M.-C. Corsi, M. Chavez, D. Schwartz, N. George, L. Hugueville, A. E. Kahn, S. Dupont, D. S. Bassett, F. D. V. Fallani, BCI learning induces core-periphery reorganization in M/EEG multiplex brain networks. *J. Neural Eng.* **18**, 056002 (2021).

20. D. R. Chialvo, Emergent complex neural dynamics. *Nature Physics*. **6**, 744–750 (2010).
21. B. Fischl, D. H. Salat, E. Busa, M. Albert, M. Dieterich, C. Haselgrove, A. Van Der Kouwe, R. Killiany, D. Kennedy, S. Klaveness, A. Montillo, N. Makris, B. Rosen, A. M. Dale, Whole brain segmentation: Automated labeling of neuroanatomical structures in the human brain. *Neuron*. **33**, 341–355 (2002).
22. A. J. Bell, T. J. Sejnowski, An information-maximization approach to blind separation and blind deconvolution. *Neural Comput*. **7**, 1129–1159 (1995).
23. F. Tadel, E. Bock, G. Niso, J. C. Mosher, M. Cousineau, D. Pantazis, R. M. Leahy, S. Baillet, MEG/EEG Group Analysis With Brainstorm. *Frontiers in Neuroscience*. **13** (2019) (available at https://www.frontiersin.org/article/10.3389/fnins.2019.00076).
24. A. Levina, V. Priesemann, Subsampling scaling. *Nat Commun*. **8**, 15140 (2017).
25. C. Destrieux, B. Fischl, A. Dale, E. Halgren, Automatic parcellation of human cortical gyri and sulci using standard anatomical nomenclature. *Neuroimage*. **53**, 1–15 (2010).

Supplementary material 1

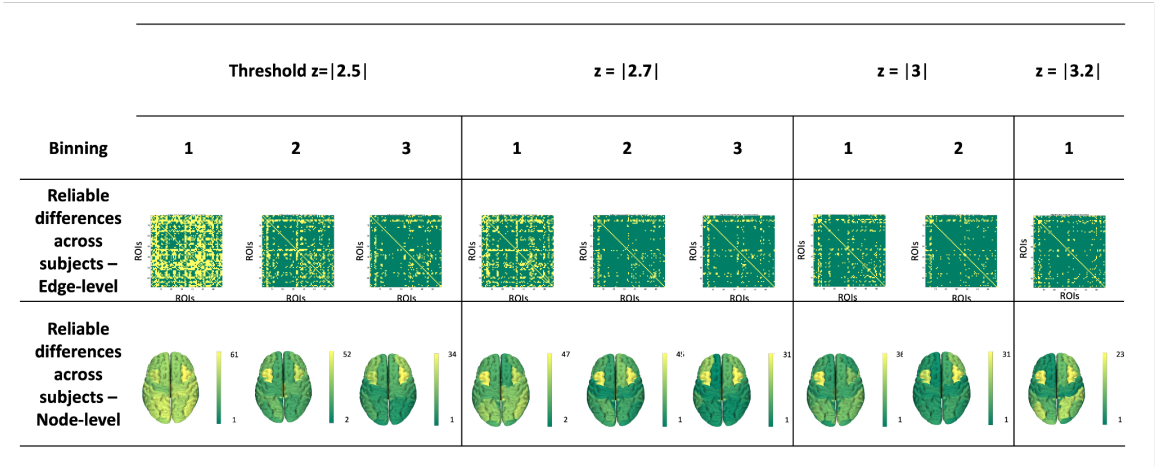

Supplementary figure 1: Replication analysis across thresholds and binnings.

Supplementary material 2

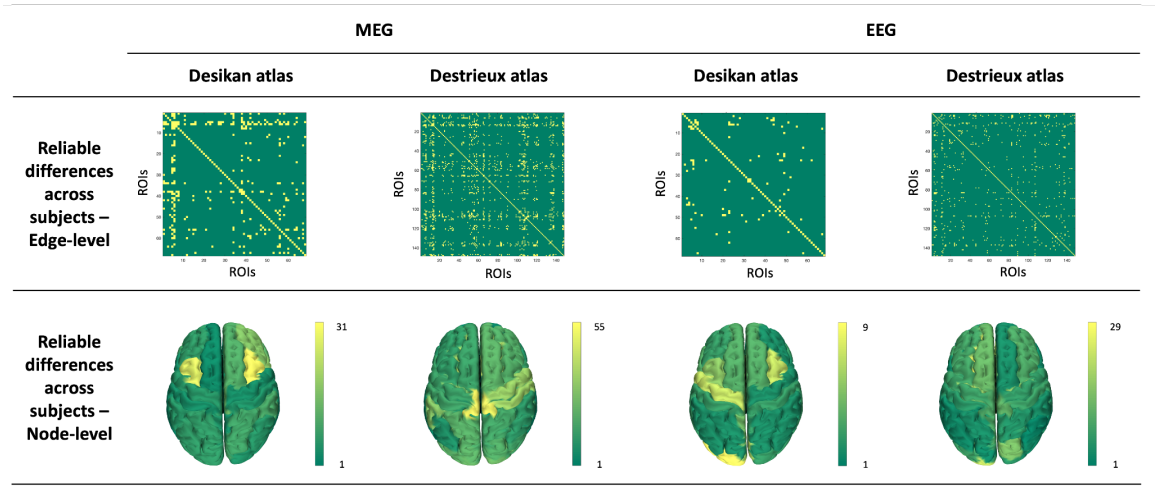

Supplementary figure 2: Replication analysis using EEG and the Destrieux atlas.

Supplementary material 3

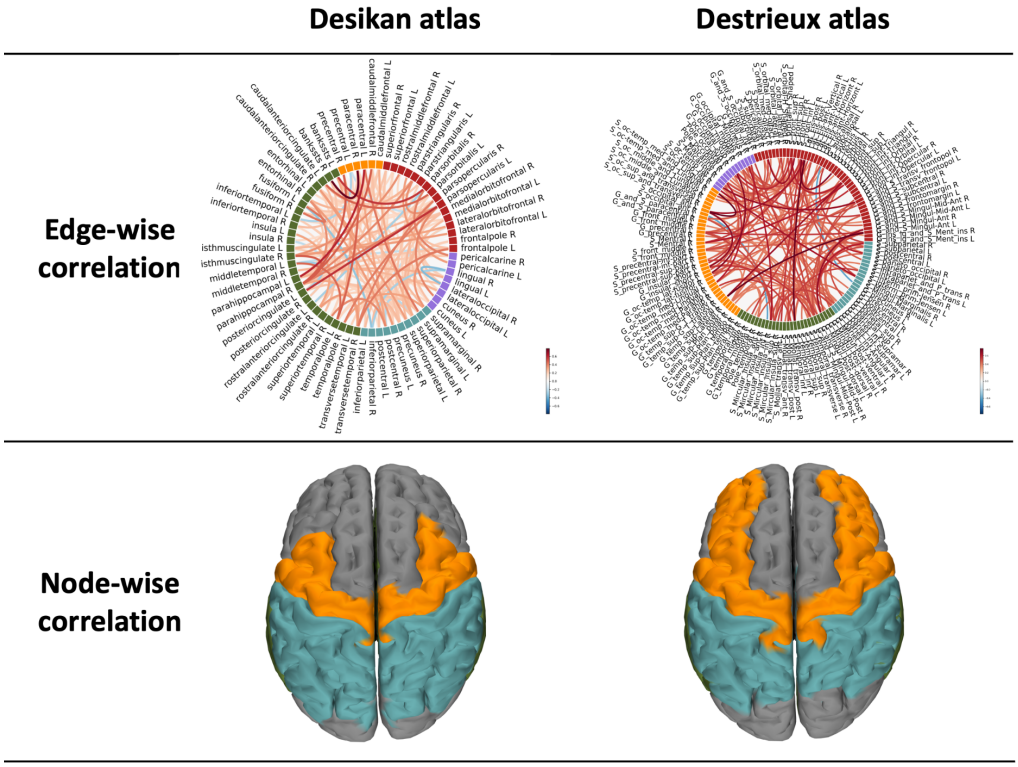

Supplementary figure 3: Replication analysis on MEG data using the Desikan and the Destrieux atlases. For visualization purposes, only the edges with |r| > 0.6 are visualized. The color of the edges is proportional to the correlation coefficient.

Supplementary material 4

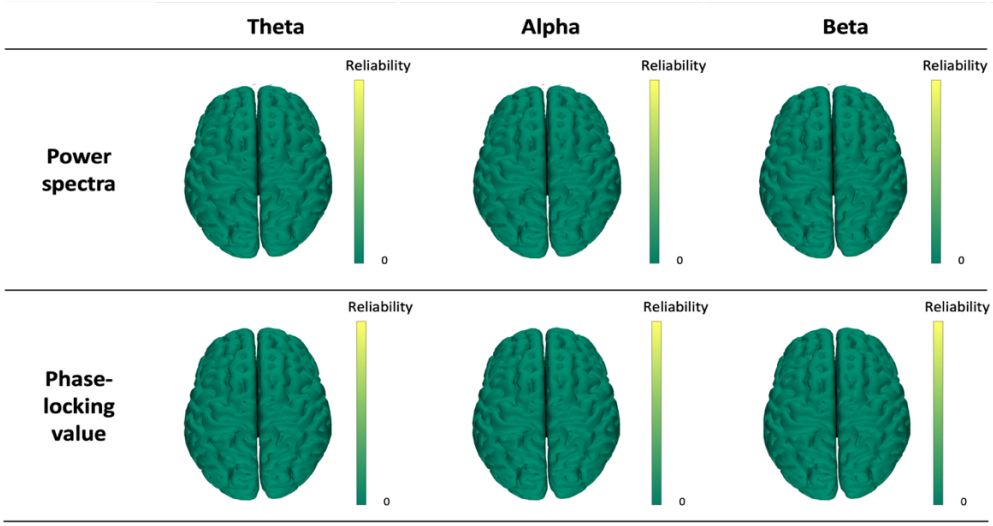

Supplementary figure 4. Reliability analysis performed on features extracted respectively via power spectra and phase-locking value estimators.